Indian Journal of Geo Marine Sciences
Vol.46 (11),November 2017, pp. 2220-2227

Dynamic analysis of an underwater suspension system in ocean currents with method of averaging

Xiang Li[1,2], Jifeng Cui[1,2], Min Zhao[1,2,*]& Tong Ge[1,2]

[1]State Key Laboratory of Ocean Engineering, Shanghai Jiao Tong University, Shanghai, 200240, China
[2]Collaborative Innovation Center for Advanced Ship and Deep-Sea Exploration (CISSE), Shanghai 200240, China

*[E-mail: min.zhao@sjtu.edu.cn]

Received 07 October 2015 ; revised 30 October 2016

Underwater suspension system is simplified into a single degree of freedom model with restoring force and quadratic damping. Nonlinear mathematical model of the suspension unit oscillating in still water and in ocean currents is established. And its analytical solutions are obtained with method of averaging. Results show that analytical solution with the method of averaging have small differences with numerical solution based on the fourth-order Runge-Kutta and can effectively describe the underwater oscillation, and solution with weaker nonlinear term has the better approximation. With large mass, short tether length and large current velocity, the analytical solution obtained with method of averaging is closer to the numerical solution.

[**Key words**: Underwater suspension system; Dynamic model; Transverse oscillation; Method of averaging; Ocean currents]

Introduction

Underwater tethered systems are vehicles, tools or other packages attached to a tether (or cable) and suspended from a surface vessel, which have been widely used in the marine environments for exploration, inspection and engineering operations[1]. They are vital tools that provide safe and effective access to deep water. Due to different aims and tasks, the tether types are various, mainly containing neutral buoyancy tether and armoured umbilical cable. Neutral buoyancy tether is mostly used on submersibles like ROV, towfish and line array sonar, and the dynamic behavior of towed object has attracted much attention from researchers[2,3,4,5,6]. Armoured umbilical cable has a submerged weight in sea water and owns greater structural strength than neutral buoyancy tether, but more motion restrictions to the suspended object, too.

The armoured umbilical cable is commonly applied in underwater suspension systems in ocean engineering, such as trencher, heavy duty ROV, TMS of ROV system, TLP foundation, heavy underwater operation tools and so on. When the underwater suspension system is lowered down into the water, vertical and transverse oscillation behaviors happen due to external excitations, which influence the safety and stability of the system. Vertical oscillation behavior subject to surface excitation has already been widely studied[7], because slack cable and large snap loads can occur during vertical oscillation behavior in rough seas, which may cause structural damage to the tether and endanger the recovery of the underwater suspension object. But less attention are paid to the transverse oscillation behavior, which is also quite important in underwater locating, time and position control of hanging work and controlling the operating range of suspension systems.

There are two kinds of modelling techniques available to predict the response of tethered systems: the continuous analytical methods and the discrete numerical models[7]. Discrete numerical models are valid for some nonlinear properties like quadratic drag and spatially varying properties of cables. The nonlinear coupling motion principle between the tether and the vehicle can be included in these models. The most prevalent numerical approaches used nowadays in determining the hydrodynamic performance of an underwater tethered system are

the lumped mass method[9], the finite difference method[10,11] and the finite element method[12,13].

Numerical methods are effective tools but they also have several limitations. For example, they need much calculation time and cannot provide quick estimates of dynamic characteristics of tethered systems[14]. But analytical methods are not constrained by these limitations. They can accurately and concisely summarizes the relationship between variables, and values of independent variables can be easily obtained through inverse calculation corresponding to the dependent variables. Driscoll et al. once developed a continuous one-dimensional analytic model which could simulate a vertically tethered system subject to surface excitation[7]. The amplitude of ship motion that triggers a snap load could be predicted by solving the transfer function of ship-cage motion.

Main purpose of this paper is to establish a nonlinear one-dimensional analytic model that represents the transverse oscillation behavior of a tethered suspension system in ocean currents, and find the analytical solution with method of averaging, which will be useful to predict the oscillation characteristics.

Materials and Methods

In the real ocean environment, the underwater suspension system usually works with the surface ship floating and the tether length varying. Its motion characteristics have great complexity. Therefore, the underwater suspension system is simplified as a pendulum to get the equation of vibration damping, and some assumptions are made as following:

- The underwater suspension object oscillates in small amplitude, namely the maximum pendulum angle is less than 5°, due to excitation forces induced by currents or ship motion through tethers;
- Without considering the tether's elastic extension, effects of gravity and flow resistance of the tether are neglected, because they are too much smaller compared to the forces directly acted on the submerged object which has too much more weight than the tether;
- Regardless of motion of the mother ship, the transport inertial force and Coriolis inertial force are zero, namely F_{Ie} = 0 and F_{IC} = 0. The change of position where the tether is connected to the surface ship is ignored.

Fig. 1 shows a typical underwater suspension system where the ship and undersea unit are connected by a long elastic tether. The system is simplified into a single degree of freedom model with restoring force and quadratic damping. In order to analyze the motion of the underwater suspension object, the coordinate frame *xoy* is first established as shown in Fig. 1, and the origin *O* is set in the center of the bottom of ship. The coordinate axis *x* is horizontal, and coordinate axis *y* is vertical and directed from top to bottom. The angular displacement between tether and coordinate axis *y* is defined as φ, which is positive when the suspension object moves to the right side of axis *y*.

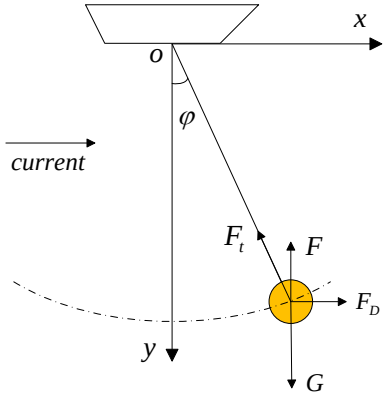

Fig. 1—Definition of coordinate system and symbols

The underwater suspension object is acted upon by the following forces[15]:

(1) Gravity $G = mg$, buoyancy $F = \rho Vg = m_f g$;

(2) Added mass force due to acceleration $m_a \frac{du}{dt}$, m_a is the added mass, u is the motion velocity of the suspension object;

(3) Tether tension F_t ;

(4) Considering the influence of ocean current, the drag force on the underwater suspension object can be written as

$$F_D = -k\left|u - u_c\cos\varphi\right|(u - u_c\cos\varphi)$$
$$= -\frac{1}{2}C_d\rho_w S\left|\frac{ds}{dt} - u_c\cos\varphi\right|\left(\frac{ds}{dt} - u_c\cos\varphi\right)$$

where C_d is drag coefficient related with Reynolds number, ρ_w is sea water density, S is projected area of the submerged object, s is the object's displacement, u_c is ocean current velocity, and φ is the small deflection angle.

Due to D'Alembert principle, the basic equation of relative motion dynamics is established, and projected to the tangent axis $\vec{t}$ of the oscillation trajectory, then we can obtain

$$m\frac{d^2s}{dt^2} = -(G - F)\sin\varphi - m_a\frac{d^2s}{dt^2}$$
$$-\frac{1}{2}C_d\rho_w S\left|\frac{ds}{dt} - u_c\cos\varphi\right|\left(\frac{ds}{dt} - u_c\cos\varphi\right) \quad \ldots(1)$$

When the suspension object makes micro-amplitude vibration, deflection angle φ is small ($\leq 5°$), and $\sin\varphi \approx \varphi$, $\cos\varphi \approx 1$, $s = \varphi l$, then Eq. (1) can be written as

$$(m+m_a)l\frac{d^2\varphi}{dt^2} = -(G-F)\varphi - \frac{1}{2}C_d\rho_w S\left|l\frac{d\varphi}{dt}-u_c\right|\left(l\frac{d\varphi}{dt}-u_c\right) \quad \ldots(2)$$

Setting damping parameter $\varepsilon = \frac{C_d\rho_w Sl}{2(m+m_a)}$ and angular frequency $\omega = \sqrt{(G-F)/(ml+m_a l)}$, Eq. (2) can be rewritten in the following form

$$\frac{d^2\varphi}{dt^2} + \omega^2\varphi = -\varepsilon\left|\frac{d\varphi}{dt}-\frac{u_c}{l}\right|\left(\frac{d\varphi}{dt}-\frac{u_c}{l}\right) \quad \ldots(3)$$

Eq. (3) is the differential equation of the underwater suspension object making micro-amplitude vibration in ocean current environment, describing the rules of oscillation with square damping. The equation has the term of ocean currents, which is the key point different from conventional simple pendulum equations. Due to the effect of the damping term, the amplitude decays constantly.

The hydrodynamic added forces and moments come about from the acceleration of the fluid particles when they encounter the submerged object. Since there is no relative acceleration in the normal direction between submerged object and its surrounding body of fluid, the normal added mass is ignored. If the forces are projected to the normal axis $\vec{n}$ of the oscillation trajectory, we can obtain the tether tension

$$F_t = m\left(\frac{d\varphi}{dt}\right)^2 l + (G-F)\cos\varphi + \frac{1}{2}C_d\rho_w S\left|\frac{d\varphi}{dt}l-u_c\right|\left(\frac{d\varphi}{dt}l-u_c\right)\sin\varphi \quad \ldots(4)$$

Solution procedures with method of averaging

In the above section, the differential equation governing the oscillation of the suspension object in ocean currents with a single degree of freedom is obtained. As the vibration equation has the term of absolute value, method of averaging is a proper way to solve and get the analytical solution[16].

As we know, if moving in ocean currents, the underwater suspension object will not oscillate around the *y* axis and will have a balance angle, which can be got from static equilibrium. If letting $\lim_{t\to\infty}\ddot{\varphi}(t) = 0$ and $\lim_{t\to\infty}\dot{\varphi}(t) = 0$ in Eq. (3), we can obtain the balance angle $\lim_{t\to\infty}\varphi(t) = \frac{\varepsilon u_c^2}{l^2\omega^2} = \frac{C_d\rho_w Su_c^2}{2(G-F)}$, which is consistent with solution by static equilibrium.

Consider the nonlinear oscillation equation of the underwater suspension object

$$\ddot{\varphi} + \omega^2\varphi = \varepsilon f(\varphi,\dot{\varphi}) \quad \ldots(5)$$

The solution can be expressed in the following form provided that a and θ are considered as functions of t rather than constants according to method of averaging. In order to describe the balance angle, a constant A is introduced. So the solution gives

$$\varphi = A + a(t)\cos[\omega t - \theta(t)] \quad \ldots(6)$$

$$\dot{\varphi} = -a(t)\omega\sin[\omega t - \theta(t)] \quad \ldots(7)$$

where

$$A = \lim_{t\to\infty}\varphi(t) = \frac{\varepsilon u_c^2}{l^2\omega^2} = \frac{C_d\rho_w Su_c^2}{2(G-F)} \quad \ldots(8)$$

and the following equations describing the slow variations of $a(t)$ and $\theta(t)$

$$\dot{a} = -\frac{\varepsilon}{2\pi\omega}\int_0^{2\pi} f(a\cos\psi, -a\omega\sin\psi)\sin\psi d\psi \quad \ldots(9)$$

$$\dot{\theta} = \frac{\varepsilon}{2\pi\omega a}\int_0^{2\pi} f(a\cos\psi, -a\omega\sin\psi)\cos\psi d\psi \quad \ldots(10)$$

where $\psi = \omega t - \theta$. Eq. (9) and Eq. (10) are called the averaging equations.

Comparing Eq. (3) and (5), we know

$$f = -\left|\frac{d\varphi}{dt}-\frac{u_c}{l}\right|\left(\frac{d\varphi}{dt}-\frac{u_c}{l}\right) = \left|a\omega\sin\psi+\frac{u_c}{l}\right|\left(a\omega\sin\psi+\frac{u_c}{l}\right) \quad \ldots(11)$$

For the underwater suspension object,

(1) In the ideal condition of still water with current velocity being zero, Eq. (11) can be written as

$$f = -\left|\frac{d\varphi}{dt}\right|\frac{d\varphi}{dt} = \left|a\omega\sin\psi\right|a\omega\sin\psi \quad \ldots(12)$$

Substituting f into Eq. (9) and Eq. (10), we obtain

$$\dot{a} = -\frac{4\varepsilon\omega a^2}{3\pi} \quad \ldots(13)$$

$$\dot{\theta} = 0 \quad \ldots(14)$$

thus

$$a = -\left(\frac{4\varepsilon\omega t}{3\pi}+C_1\right)^{-1} \quad \ldots(15)$$

$$\theta = C_2 \quad \ldots(16)$$

so we have

$$\varphi = -\left(\frac{4\varepsilon\omega t}{3\pi} + C_1\right)^{-1} \cos(\omega t - C_2) \quad \ldots(17)$$

where C_1 and C_2 are undetermined parameters.

In general, giving initial conditions $\varphi(0) = \varphi_0$ and $\dot{\varphi}(0) = 0$, substituting them into Eq. (17), C_1 and C_2 yield

$$C_1 = -\frac{\sqrt{-16\varepsilon^2\varphi_0^2 + 9\pi^2}}{3\pi\varphi_0}, \quad C_2 = -\arccos\left(\frac{\sqrt{-16\varepsilon^2\varphi_0^2 + 9\pi^2}}{3\pi}\right) \quad \ldots(18)$$

or

$$C_1 = \frac{\sqrt{-16\varepsilon^2\varphi_0^2 + 9\pi^2}}{3\pi\varphi_0}, \quad C_2 = -\arccos\left(-\frac{\sqrt{-16\varepsilon^2\varphi_0^2 + 9\pi^2}}{3\pi}\right) \quad \ldots(19)$$

Substituting Eq.(18) into Eq. (17) makes the divergence of φ in the initial time, not satisfying the physical scene, thus abandoning Eq.(18).

(2) Considering the ocean current condition, the value of $\frac{u_c}{a\omega l} = \frac{u_c}{a}\sqrt{\frac{m+m_a}{(G-F)l}}$ influences the absolute value symbol of Eq. (11). As the amplitude maximum is generally 5°, if the ocean current velocity is large and tether length is short, $\frac{u_c}{a\omega l}$ can be larger than 1, and Eq. (11) can be rewritten as

$$f = -\left|\frac{d\varphi}{dt} - \frac{u_c}{l}\right|\left(\frac{d\varphi}{dt} - \frac{u_c}{l}\right) = \left(a\omega\sin\psi + \frac{u_c}{l}\right)^2 \quad \ldots(20)$$

Substituting *f* into (9) and (10), we have

$$\dot{a} = -\frac{u_c\varepsilon a}{l} \quad \ldots(21)$$

$$\dot{\theta} = 0 \quad \ldots(22)$$

Thus we obtain

$$a = C_1 e^{-u_c\varepsilon t/l} \quad \ldots(23)$$

$$\theta = C_2 \quad \ldots(24)$$

hence,

$$\varphi = \frac{\varepsilon u_c^2}{l^2\omega^2} + C_1 e^{\frac{-u_c\varepsilon}{l}t}\cos(\omega t - C_2) \quad \ldots(25)$$

where C_1 and C_2 are undetermined parameters.

Giving initial conditions $\varphi(0) = \varphi_0$ and $\dot{\varphi}(0) = 0$, and substituting them into Eq. (25), C_1, C_2 can be got as

$$C_1 = -\frac{l^4\omega^4\varphi_0 - l^2\omega^2\varepsilon u_c^2 + l^2\omega^2\varepsilon^2\varphi_0 u_c^2 - \varepsilon^3 u_c^4}{l^3\omega^3\sqrt{l^2\omega^2 + \varepsilon^2 u_c^2}}, \quad C_2 = -\arccos\left(-\frac{l\omega}{\sqrt{l^2\omega^2 + \varepsilon^2 u_c^2}}\right) \quad \ldots(26)$$

or

$$C_1 = \frac{l^4\omega^4\varphi_0 - l^2\omega^2\varepsilon u_c^2 + l^2\omega^2\varepsilon^2\varphi_0 u_c^2 - \varepsilon^3 u_c^4}{l^3\omega^3\sqrt{l^2\omega^2 + \varepsilon^2 u_c^2}}, \quad C_2 = \arccos\left(\frac{l\omega}{\sqrt{l^2\omega^2 + \varepsilon^2 u_c^2}}\right) \quad \ldots(27)$$

The above parameter group satisfies the physical scene, but C_1 has opposite sign in (26) and (27), C_2 in (26) differs by a phase of π from (27). If considering C_2 varying between $-\pi/2 \le C_2 \le \pi/2$, the parameters in (26) can be abandoned.

Eq. (17) and Eq. (25) are the approximate analytical solutions, and C_1, C_2 adopt the parameters in (19) and (27) respectively.

It can be seen from Eq. (13) and Eq. (21) that initially the rate at which the amplitude of the response decreases is proportional to the square of the amplitude of the initial disturbance in still water and to the amplitude of the initial disturbance in ocean currents. Thus when the amplitude of the initial disturbance is large, the initial decay is slower in still water than in ocean currents. If the initial disturbance is small, the opposite is expected to be true.

According to Eq. (17) and Eq. (25), the amplitude in still water decays algebraically, while the amplitude in ocean currents decays exponentially with time. Given initial parameters and ocean current conditions, when $t \to \infty$, amplitude *a* tends to 0, without relationship with initial φ_0. θ keeps constant, resulting that the solution with the method of averaging for the first order approximation has no modification on the oscillation frequency.

Results and Discussions

Different parameters are given to the analytical expressions to analyze the effects of the different types of damping, and validate the analytical solution for cases with and without ocean currents. For simplicity,

$C_d = 1.05$, $m_f = 0.5m$, $m_a = 0.5m_f$. The initial conditions give $\varphi(0) = 5\pi/180$, $\dot{\varphi}(0) = 0$.

Oscillation in still water

Results of analytical solution with the method of averaging and numerical solution based on the fourth-order Runge-Kutta are compared and presented as below (solid and dotted lines, respectively). Runge-Kutta method is an effective explicit or implicit iterative method for solving nonlinear ordinary differential equation, and it has high fidelity for nonlinear solution. The small difference between analytical and numerical results shows the effectiveness of the method of averaging. The nonlinear term is determined by both damping parameter and relative angular velocity. Although the damping parameter is larger than one, with the small term of relative angular velocity, the analytical solution still has a relative satisfied approximation.

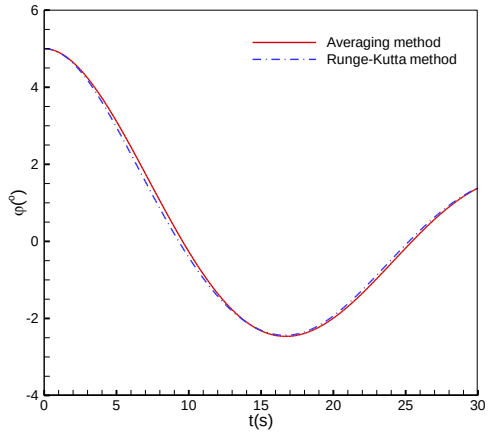

(a) Oscillation during the first 30 seconds

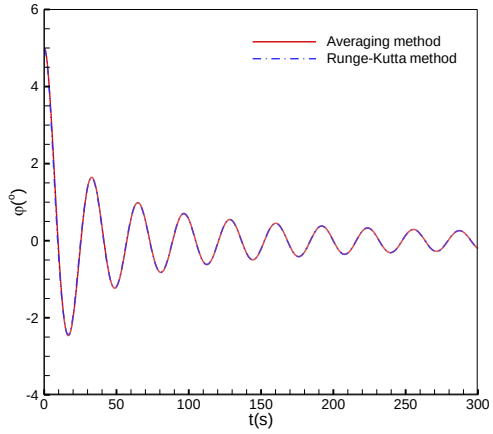

(b) Oscillation during the 300 seconds

Fig. 2—Comparison between analytical solution and numerical solution based on the fourth-order Runge-Kutta in a short time and a long time (m=100 t, l=100 m, u_c=0 m/s, ε=8.610, ω= 0.198).

Oscillation in ocean currents

The relationships between deflection angle and time with different mass are plotted in Fig. 3, and results obtained from analytical solution are compared with numerical results. As shown in the graph, the calculated values of deflection angle with method of averaging have a similar trend to those of numerical results, but the amplitude of numerical results are smaller than analytical ones. With the increase of time, deflection angle first oscillates, and then gradually damps into a steady angle. The steady angle with both averaging and Runge-Kutta method is almost the same. As the mass increases, the difference between deflection angles obtained with method of averaging and numerical method becomes smaller due to the smaller damping parameter ε. The oscillating period T keeps the same, but the deflection angle damps faster to steady status with the smaller mass.

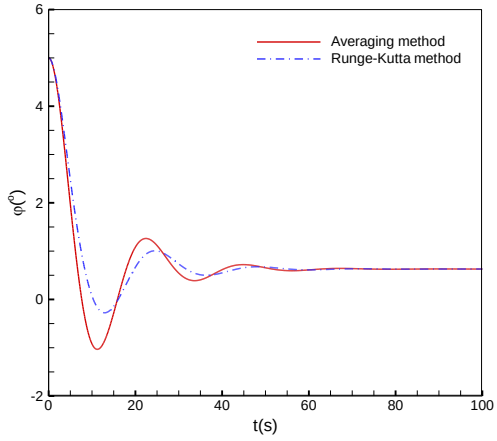

(a) m=50 t, ε=8.610, ω=0.280

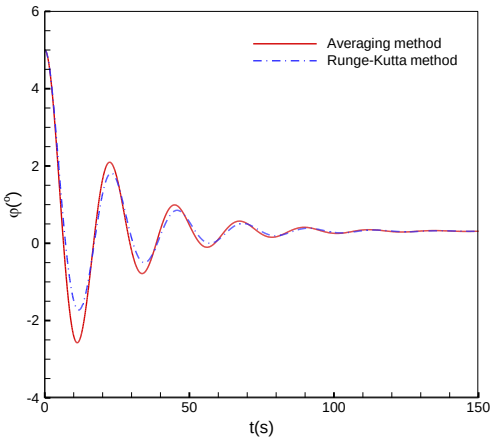

(b) m=100 t, ε=4.305, ω=0.280

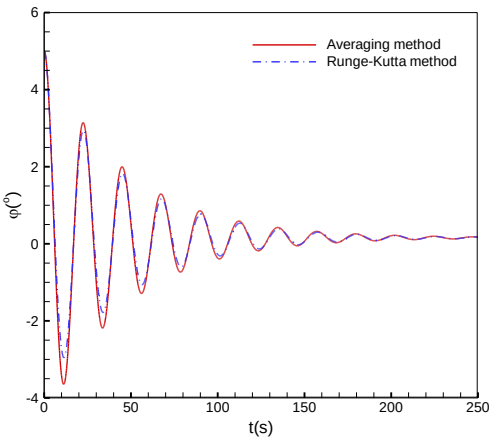

(c) m=200 t, ε=2.153, ω=0.280

Fig. 3—Deflection angle vs time with different mass (l=50 m, u_c=0.5 m/s).

Fig. 4 shows the relationships between deflection angle and time with different tether length. It can be seen that the amplitude of numerical results are smaller than analytical ones. As the tether length increases, the damping parameter ε grows larger and the difference of deflection angle obtained with method of averaging becomes bigger from those with numerical method. Since the oscillating period gives $T = 2\pi\sqrt{(m+m_a)l/(G-F)}$, the oscillating period T increases with longer tether length, which is obvious in Fig. 4. Besides, the deflection angle damps to steady status with similar time of 200s for both methods. In short, tether length influences both the damping parameter ε and period T.

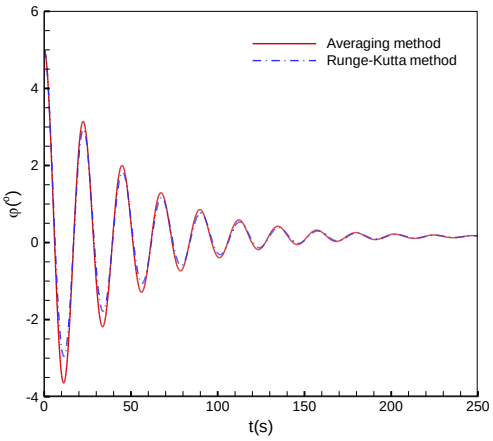

(a) l=50 m, ε=2.153, ω=0.280

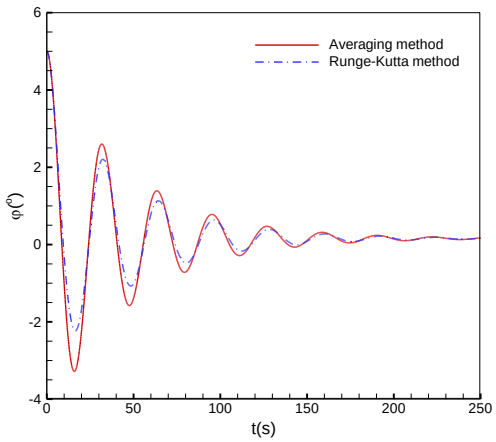

(b) l=100 m, ε=4.305, ω=0.198

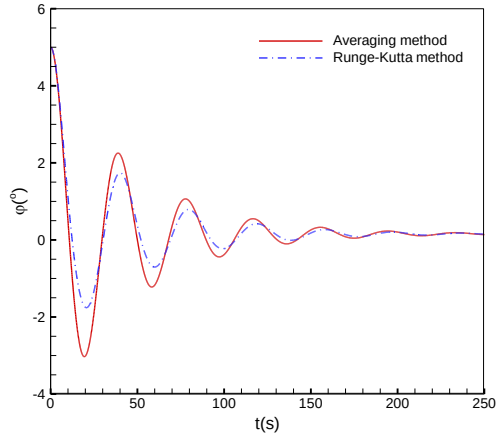

(c) l=200 m, ε=8.610, ω=0.140

Fig. 4—Deflection angle vs time with different tether length (m=200t, u_c=0.5 m/s).

Considering the influence of ocean current, the results of different current velocities obtained from analytical solution are compared with numerical results and plotted in Fig. 5. The comparison shows that the deflection angle damps to steady status in a shorter time with stronger current velocity, although the oscillating period keeps the same.

According to the equation in section 2, ocean current doesn't influence the damping parameter ε. So the deflection angles obtained with method of averaging and Runge-Kutta method have similar accuracy in environment of different ocean current velocities.

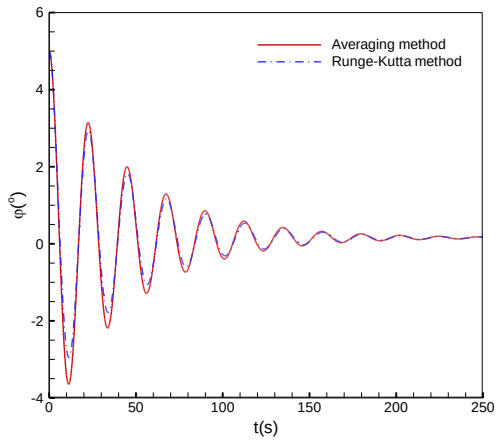

(a) u_c = 0.5 m/s, ε=2.153, ω=0.280

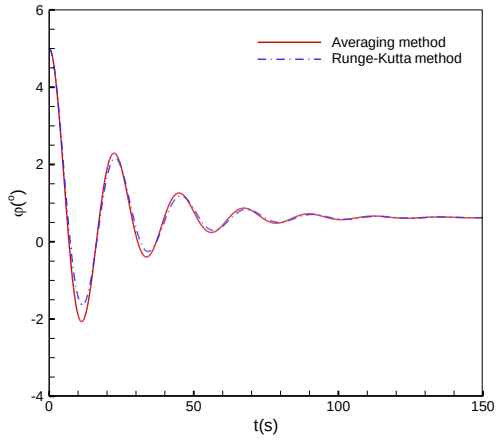

(b) u_c = 1 m/s, ε=2.153, ω=0.280

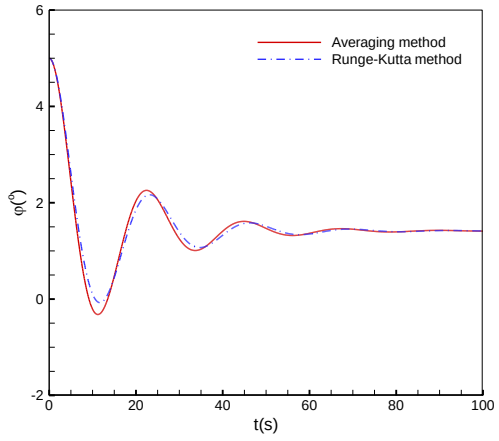

(c) u_c = 1.5 m/s, ε=2.153, ω=0.280

Fig. 5—Deflection angle vs time with different ocean current velocity (m=200t, l=50m).

Conclusions

The amplitude attenuation is sensitive to variation of the damping parameter ε, which is affected by some physical properties, like the mass, tether length and current velocity. With large mass, short tether length and large current velocity, the analytical solution obtained with method of averaging is closer to the numerical solution. The nonlinear term is determined by both damping parameter and relative angular velocity. The analytical solution with weaker nonlinear term has the better approximation. Method of averaging has only a first-order approximate precision of solving nonlinear equation. But for this model, method of averaging can be simple and effective to solve the problem, and result in satisfactory accuracy. If more accurate analytical solutions are required, other analytical methods need to be tried. The oscillation model built in this paper is relatively ideal, and some conditions like the elasticity, gravity and drag force of tether are ignored, which exist in practical problems and can be studied further.

Acknowledgements

The support of High Technology Ship Research and Program of Ministry of Industry and Information Technology of the People's Republic of China (Grant No. 539 [2012]), and the Specialized Research Fund for the Doctoral Program of Higher Education of China (Grant No. 20120073120014) for this work is gratefully acknowledged.

References

1 Lueck, R.G., Driscoll, F.R. and Nahon, M., A wavelet for predicting the time-domain response of vertically tethered systems, *Ocean Eng.*, 2000, 27(12):1441-1453.

2 Fang, M.C., Chen, J. H., Luo, J. H. and Hou, C.S., On the behavior of an underwater remotely operated vehicle in a uniform current, *Marine Technol.*, 2008, 45(4):241-249.

3 Zhu, K.Q., Zheng, D.C., Cai, Y., Yu, C.L., Wang, R., Liu, Y.L., and Zhang, F., Nonlinear hydrodynamic response of marine cable-body system under random dynamic excitations, *J. Hydrodyn., Ser. B*, 2009, 21(6):851-855.

4 Shin, H.K., Ryue, J.S., Ahn, H.T., Seo, H.S. and Kwon, O.C., Study on dynamic behavior analysis of towed line array sensor, *Int. J. Nav. Architect. Ocean Eng.*, 2012, 4(1): 10-20.

5 Yu, S.C., Yuh, J. and Kim, J., Armless underwater manipulation using a small deployable agent vehicle connected by a smart cable, *Ocean Eng.*, 2013, 70:149-159.

6 Park, J. and Kim, N., Dynamics modeling of a semi-submersible autonomous underwater vehicle with a towfish towed by a cable, *Int. J. Nav. Architect. Ocean Eng.*, 2015, 7(2):409-425.

7 Driscoll, F.R., Lueck, R.G. and Nahon, M., The motion of a deep-sea remotely operated vehicle system, Part 2: analytic model, *Ocean Eng.*, 2000, 27(1): 57-76.

8 Driscoll, F.R., Lueck, R.G. and Nahon, M., Development and validation of a lumped-mass dynamics model of a deep-sea ROV system, *Appl. Ocean Res.*, 2000, 22(3):169-182.

9 Walton, T.S. and Polachek, H., Calculation of transient motion of submerged cables, *Math. Comput.*, 1960, 14(69):27-46.

10 Sanders, J.V., A three dimensional dynamic analysis of a towed system, *Ocean Eng.*, 1982, 9(5):483-499.

11 Ablow, C.M. and Schechter, S., Numerical simulation of undersea cable dynamics, *Ocean Eng.*, 1983, 10(6):443-457.

12 Leonard, J.W., Nonlinear dynamics of cables with low initial tension, *J. Eng. Mech. Div.*, 1972, 98(2): 293-309.

13 Ma, D.C.C., Chu, K.H. and Leonard, J.W., Slack-elasto-plastic dynamics of cable system, *J. Eng. Mech. Div.*, 1979, 105(2):207-222.

14 Zhu, K.Q., Zhu, H.Y., Zhang, Y.S. and Gao, J., A multi-body space-coupled motion simulation for a deep-sea tethered remotely operated vehicle, *J. Hydrodyn., Ser. B*, 2008, 20(2): 210-215.

15 Fossen, T. I., *Guidance and control of ocean vehicles*, John Wiley & Sons, 1994.

16 Nayfeh, A.H., *Introduction to perturbation techniques*, John Wiley & Sons, 2011.